



Contents lists available at ScienceDirect

## Bioorganic &amp; Medicinal Chemistry Letters

journal homepage: [www.elsevier.com/locate/bmcl](http://www.elsevier.com/locate/bmcl)

# Adamantyl- and other polycyclic cage-based conjugates of desferrioxamine B (DFOB) for treating iron-mediated toxicity in cell models of Parkinson's disease



Thomas J. Telfer<sup>a,d</sup>, Jeffrey R. Liddell<sup>b,d</sup>, Clare Duncan<sup>b</sup>, Anthony R. White<sup>b,c</sup>, Rachel Codd<sup>a,\*</sup>

<sup>a</sup> School of Medical Sciences (Pharmacology) and Bosch Institute, The University of Sydney, New South Wales 2006, Australia

<sup>b</sup> Department of Pathology, The University of Melbourne, Victoria 3010, Australia

<sup>c</sup> Cell and Molecular Biology, QIMR Berghofer Medical Research Institute, Herston, Queensland 4006, Australia

## ARTICLE INFO

## Article history:

Received 24 January 2017

Revised 28 February 2017

Accepted 1 March 2017

Available online 2 March 2017

## Keywords:

Desferrioxamine B

Polycyclic cage compounds

Iron chelators

Parkinson's disease

## ABSTRACT

The death of dopaminergic neurons is a major pathological hallmark of Parkinson's disease (PD). Elevated iron within the substantia nigra of the PD brain is thought to catalyze this neuronal death through hydroxyl radical-derived oxidative damage. Removing this excess iron presents a potential therapeutic strategy for PD. Seventeen derivatives of the non-toxic iron chelator desferrioxamine B (DFOB) were prepared by the conjugation of adamantyl- (**1–4**, **8–12**), deconstructed adamantyl units (**5–7**), norborna(e)ne- (**13–16**) or bicyclo[2.2.2]octane-based (**17**) ancillary fragments to the terminal amine group. The range of experimental  $\log P$  values of **1–17** ( $\log P = 0.15–2.82$ ) was greater than water soluble DFOB ( $\log P = -2.29$ ), with the increased hydrophobicity designed to improve cell membrane carriage to facilitate intracellular iron sequestration. The first activity screen showed compounds with methyl-substituted adamantyl (**1–3**), noradamantyl (**5**), or 1-pentylbicyclo[2.2.2]octane (**17**) ancillary groups significantly rescued iron-mediated oxidative stress in confluent PD-relevant SK-N-BE2-M17 neuroblastoma cells (M17 cells) exposed to 1,1'-dimethyl-4,4'-bipyridinium (paraquat, PQ) or  $H_2O_2$ . The second dose-dependence screen ranked **1–3** and **17** as the top candidates ( $EC_{50} \sim 10 \mu M$ ) in the rescue of PQ-treated M17 cells. The ancillary fragments of **1–3** and **17** clustered in a region defined by a close-to-zero dipole moment,  $\log P$  values of 2–2.8 and a surface area:volume ratio of 0.60–0.61. Results of iron leaching studies indicate that the compounds may be operating via mechanisms beyond solely removing intracellular iron. The DFOB conjugates with methyl-substituted adamantyl ancillary groups (**1–3**) were the top and most consistent performers in this class of compound designed for PD.

© 2017 Elsevier Ltd. All rights reserved.

The concentration of iron in humans is necessarily tightly regulated due to the absence of active iron excretory mechanisms.<sup>1</sup> Excess iron can catalyze the production of reactive oxygen species (ROS), which can damage DNA, RNA, proteins and lipids, as a contributing factor to the pathogenesis of a number of conditions.<sup>2</sup> In transfusion-dependent iron overload disease, which occurs in people with inherited hemoglobin disorders including beta-thalassemia and sickle cell anemia, excess iron is initially accumulated in the plasma and ultimately in the organs.<sup>3–5</sup> In Parkinson's disease (PD), excess iron accumulates in the pars compacta of the substantia nigra (SNpc) region of the brain, with the effects widely believed to contribute to the death of dopaminergic neurons, as one of the hallmarks of the condition.<sup>6</sup> Due to the aging population,

the incidence of PD world-wide is expected to double by 2030 to 9.3 million people,<sup>7</sup> which highlights the need to identify agents that could offer neuroprotective potential. Evidence to support iron as a PD therapeutic target has been provided from a clinical study using the synthetic iron chelator deferiprone, which is in use for iron overload disease.<sup>8</sup> The iron chelator desferrioxamine B (DFOB, Fig. 1,  $R = H$ ), which is a secondary metabolite produced by many *Streptomyces* species for iron acquisition,<sup>9,10</sup> is another agent used to treat iron overload disease. As evolved by nature, DFOB has a high affinity and selectivity for Fe(III) ( $\log K_{Fe(III)} = 30$ ,  $\log K_{Fe(II)} = 8$ ), and its water solubility ( $\log P = -2.10$ ) is well matched with its first-line function to remove iron from plasma. DFOB has limited ability to cross the blood-brain barrier. To expand potential therapeutic options for iron chelation in PD, the current work prepared analogues of non-toxic DFOB with increased hydrophobicity to improve cell membrane carriage. Methods to positively modulate the cell carriage of DFOB is of increasing interest.<sup>11,12</sup> Previous

\* Corresponding author.

E-mail address: [rachel.codd@sydney.edu.au](mailto:rachel.codd@sydney.edu.au) (R. Codd).<sup>d</sup> Contributed equally to the work.

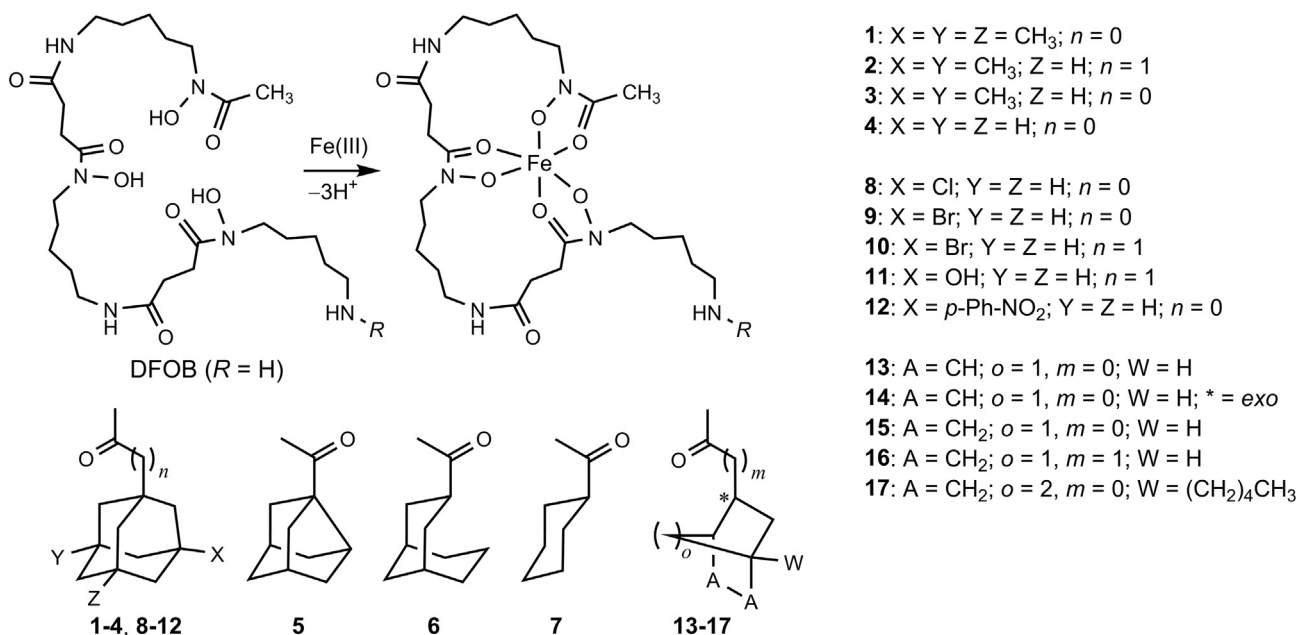


Fig. 1. Compounds prepared in this study.

work characterized a small group of conjugates between DFOB and lipophilic ancillary fragments, including adamantyl motifs.<sup>13</sup> The adamantyl group and other caged-based motifs can positively modulate drug properties, with these groups present in many clinical agents.<sup>14–16</sup> Several candidates from the first generation group showed promise in a series of *in vitro* PD cell models.<sup>17</sup> This study sought to rank the performance of new and known candidates before progressing further along the clinical pipeline to *in vivo* studies.

Compounds **1–17** (Fig. 1) were prepared from a methanol (10 mL) reaction solution containing DFOB (0.325 mmol), the NHS-activated ester of the relevant ancillary fragment (0.325 mmol), and NaOH (0.05 mmol), which was stirred at reflux (70 °C, 3 h). The

solvent was removed *in vacuo*, and the solid was washed with diethylether (5 × 5 mL) and water (5 × 5 mL), followed by purification to >95% (CHN microanalysis) by semi-preparative reverse-phase HPLC (Supplementary Information). The integrity of 1:1 Fe (III) coordination for **1–17** was confirmed from LC-MS measurements of Fe(III) complexes, which analyzed as [M+H]<sup>+</sup> and [M+2H]<sup>2+</sup> adducts (Table S1).

The log*P* values of **1–17** (Table 1) were estimated from the RP-HPLC retention time of the compound (*t<sub>R</sub>*) and the deadtime (*t<sub>0</sub>*), using the formulae:  $k = (t_R - t_0)/t_0$ ; and  $\log k = a + b \log P$ , with the use of the standard calibrants: dimethyl phthalate (log*P* = 1.59), diethyl phthalate (log*P* = 2.48), naphthalene (log*P* = 3.27) and dibenzofuran (log*P* = 3.76).<sup>18,19</sup> The use of this method was

Table 1

Chromatographic data and log*P* values (experiment, calculated) for DFOB and **1–17** and parameters (log*P*, dipole, oval, polarizability, surface area:volume ratio) of the ancillary fragments.

No	[M]	<i>t<sub>R</sub></i> (min)	$\Delta t_{R [Fe(III)]}$ (min) <sup>a</sup>	log <i>P</i> <sup>b</sup>	clog <i>P</i> <sup>c</sup>	clog <i>P<sub>F</sub></i> <sup>d</sup>	Dipole <sub>F</sub> <sup>d</sup> (D)	Oval <sub>F</sub> <sup>e</sup>	Polar <sub>F</sub> <sup>d</sup> (Å <sup>3</sup> )	SA/V <sub>F</sub> <sup>d</sup> (Å <sup>-1</sup> )
DFOB	560.4	10.70	-0.52	-2.29	-0.18	N/A	N/A	N/A	N/A	N/A
<b>1</b>	764.5	22.14	1.85	2.54	3.62	3.99	0.01	1.28	22.31	0.60
<b>2</b>	764.5	21.49	1.54	2.17	4.76	3.99	0.01	1.28	22.31	0.60
<b>3</b>	750.5	20.83	1.06	2.07	3.10	3.56	0.01	1.24	20.47	0.61
<b>4</b>	722.5	18.51	0.43	1.32	2.06	2.69	0	1.17	16.8	0.64
<b>5</b>	708.4	17.51	0.48	0.98	1.50	2.3	0.1	1.16	14.97	0.66
<b>6</b>	710.5	18.43	0.65	1.87	2.83	2.93	0.05	1.18	15.74	0.64
<b>7</b>	670.4	16.06	-0.04	0.96	1.43	2.38	0	1.16	11.01	0.71
<b>8</b>	756.4	18.61	0.83	1.84	2.04	2.6	1.81	1.21	18.73	0.63
<b>9</b>	800.4	19.24	0.91	1.90	2.18	2.66	2.16	1.21	19.43	0.62
<b>10</b>	814.4	19.53	1.09	1.84	3.69	3.1	2.18	1.25	21.26	0.61
<b>11</b>	752.5	14.74	-0.52	0.15	0.59	1.89	1.53	1.23	19.27	0.62
<b>12</b>	843.5	21.17	1.71	2.09	3.21	4.18	6.04	1.35	28.18	0.60
<b>13<sup>f</sup></b>	680.4	15.64	-0.32	1.40	1.22	2.01	0.17	1.13	11.88	0.69
<b>14<sup>f</sup></b>	680.4	16.22	0	0.50	1.22	2.01	0.17	1.13	11.88	0.69
<b>15<sup>f</sup></b>	682.4	16.29	0.08	0.55	1.71	2.14	0.01	1.15	12.07	0.68
<b>16<sup>f</sup></b>	696.4	17.33	0.27	1.16	2.33	2.47	0.03	1.19	13.91	0.67
<b>17<sup>f</sup></b>	766.5	23.83	3.67	2.82	4.38	4.55	0.06	1.35	23.08	0.61

<sup>a</sup> *t<sub>R</sub>* (Fe(III)-complex) – *t<sub>R</sub>* (free ligand).

<sup>b</sup> Log*P*<sub>exp</sub> values estimated from RP-HPLC retention time (*t<sub>R</sub>*).

<sup>c</sup> Log*P*<sub>calc</sub> values of full molecules from ChemBioDraw Ultra 14.0.

<sup>d</sup> Calculated values (subscript 'F') of ancillary fragments excluding the carboxylic acid group (HyperChem 7.0).

<sup>e</sup> Calculated values (subscript 'F') of ancillary fragments excluding the carboxylic acid group (Spartan 10).

<sup>f</sup> Calculated values are given for *exo*-conformers. Values did not differ significantly for *endo*-conformers.

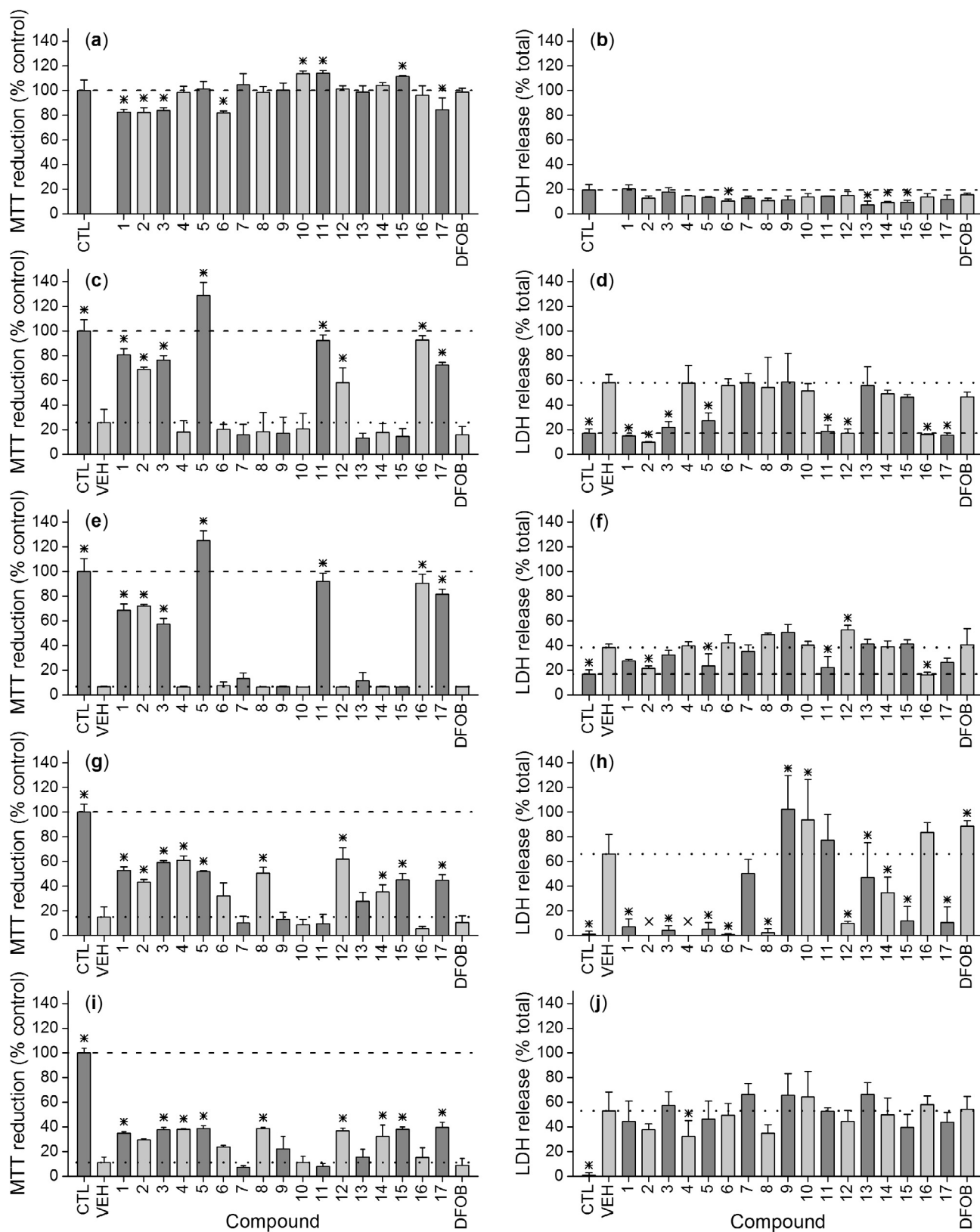


**Fig. 2.** Cell viability of confluent M17 cells treated with (a, b) DFOB (1 mM) or 1–17 (100  $\mu$ M); or upon a 2 h pre-treatment with DFOB (100  $\mu$ M) or 1–17 (100  $\mu$ M) and subsequent 24 h incubation with (c, d) PQ (1 mM) or (e, f) H<sub>2</sub>O<sub>2</sub> (1 mM); or following a 2 h pre-incubation with (g, h) PQ (2 mM) or (i, j) H<sub>2</sub>O<sub>2</sub> (0.8 mM) with a subsequent 24 h post-treatment with DFOB (100  $\mu$ M) or 1–17 (100  $\mu$ M), as measured using an MTT assay (a, c, e, g, i) or an LDH assay (b, d, f, h, j). In panel h, 2 and 4 were not tested (X), due to insufficient material. Experiments were performed twice and data are presented as averages  $\pm$  standard deviation of triplicate wells from a representative experiment, with \*P < 0.05 compared to the vehicle (VEH: stressor with no compound (dotted line)). The dashed line represents the control (CTL: no stressor and no compound).

justified due to the structural similarity of the compounds, and the absence of any log*D* contributions to the measurements for neutral **1–17** under the acid conditions (pH ~4) of the RP-HPLC procedure.<sup>13</sup> Log*P* values were determined using the more labor-intensive shake-flask method for the sub-set **1**, **3** and **4**, which gave values in reasonable agreement with those estimated from RP-HPLC. Values of a range of physicochemical measures were calculated for the ancillary fragments alone (Table 1).

Three structure-activity concepts were considered in this work. The first concept aimed to examine the optimal methylation pattern of the adamantyl group (1,3,5-trimethyl, **1**; 3,5-dimethyl, **3**,

no methyl groups, **4**) and the effects of systematically deconstructing the adamantyl group into simpler fragments, including the noradamantyl group (**5**), two fused cyclohexane groups (**6**) or cyclohexane (**7**). *n*-Hexane was also examined as an ancillary fragment, however, the DFOB-*n*-hexane conjugate was intractable and was unable to be obtained in yields that allowed biological testing. The compound assembled from 3,5-dimethyladamantylacetic acid (**2**) was also included as a structural isomer of **1** in this sub-group (group (i)). The second concept was to examine compounds that contained halogen-substituted adamantyl (acetyl) (**8–10**) or groups, or substitution with other motifs, including the hydroxyl

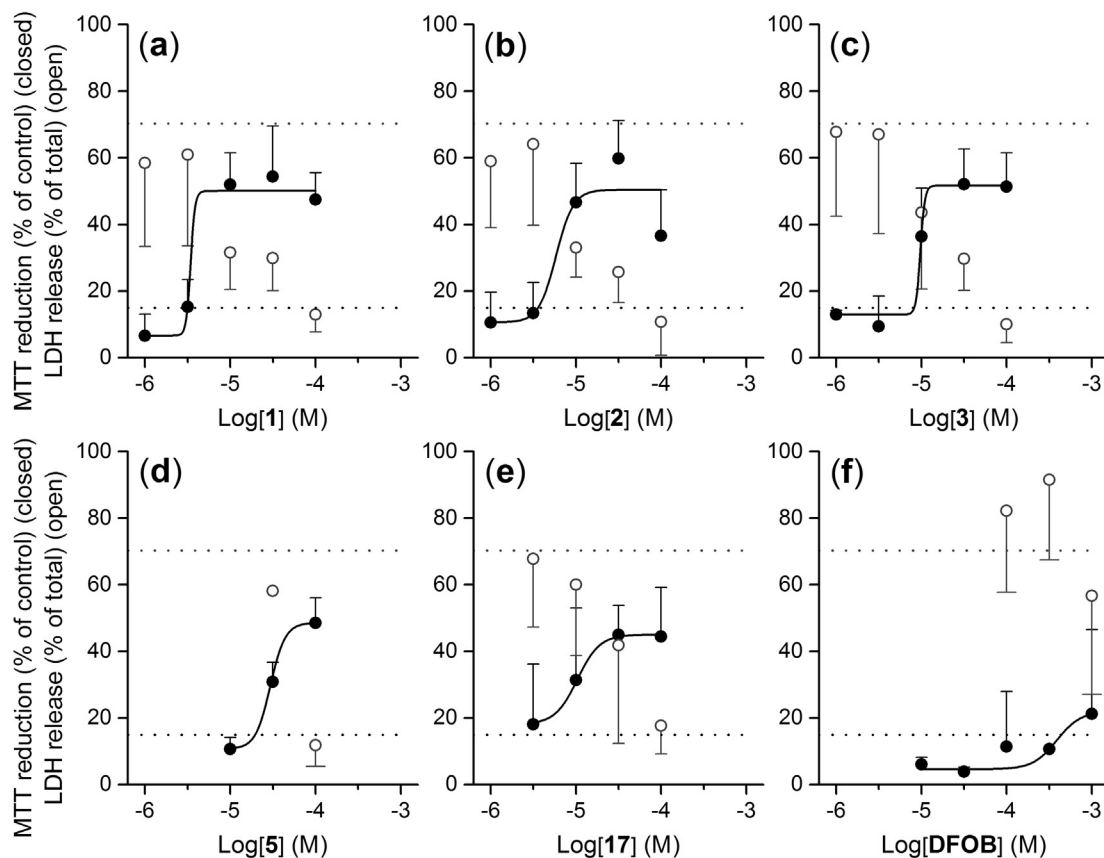


**Fig. 3.** Cell viability of confluent M17 cells pre-incubated with 2 mM PQ for 2 h, followed by post-treatment with variable concentrations of: (a) **1**, (b) **2**, (c) **3**, (d) **5**, (e) **17**, or (f) DFOB, as measured using the MTT assay (closed circles) or the LDH assay (open circles). The MTT data were fitted with dose-response curves. Responses of the PQ-treated cells in the absence of any compound (vehicle) are shown as the dotted lines for the MTT assay (black) or the LDH assay (grey). Data are presented as averages  $\pm$  standard deviation of 2–6 independent experiments.

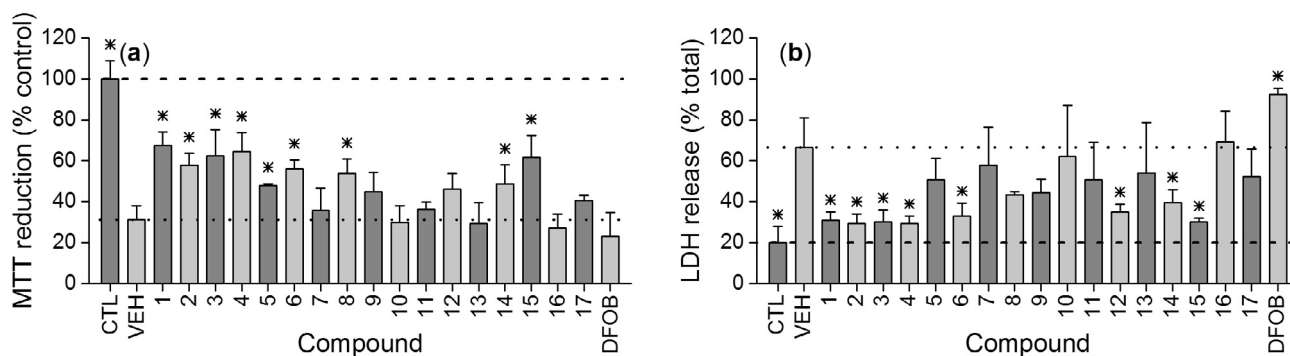


**Fig. 4.** Cell viability of confluent M17 cells pre-treated with FeCl<sub>3</sub> (200  $\mu$ M), then PQ (1 mM), then DFOB (100  $\mu$ M) or **1–17** (100  $\mu$ M) for 24 h, as measured using an MTT assay (a) or an LDH assay (b). Data are presented as averages  $\pm$  standard deviation of 3 independently prepared cell cultures, with  $P < 0.05$  compared to the vehicle (VEH: stressor with no compound (dotted line)). The dashed line represents the control (CTL: no stressor and no compound).

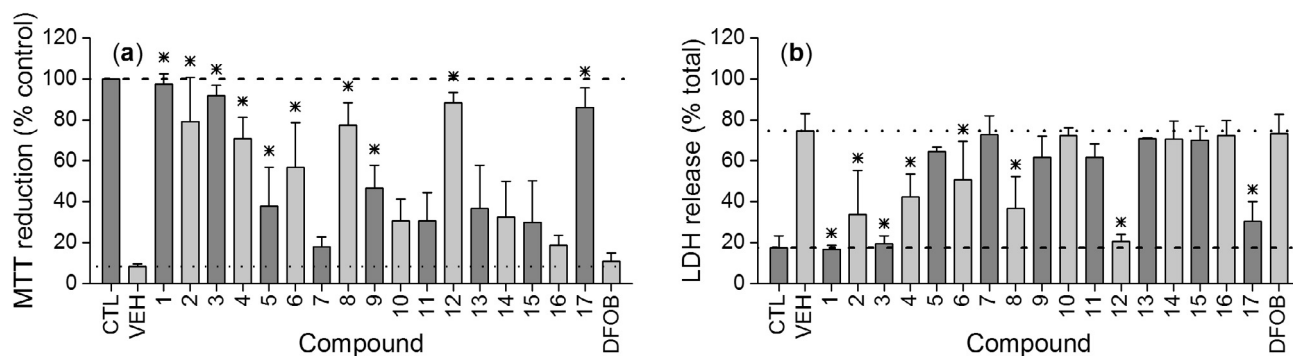


**Fig. 5.** Cell viability of primary astrocytes pre-treated with BSO for 24 h, followed by a 2-h treatment with DFOB (10  $\mu$ M) or **1–17** (10  $\mu$ M) and a subsequent 24 h incubation with 0.2 mM  $H_2O_2$ , as measured using an MTT assay (a) or an LDH assay (b). Data are presented as averages  $\pm$  standard deviation of 3 independently prepared cell cultures, with \* $P < 0.05$  compared to the vehicle (VEH: stressor with no compound (dotted line)). The dashed line represents the control (CTL: no stressor and no compound).

group (**11**) or *para*-nitrobenzene (**12**) (group (ii)). The third concept was to establish the performance of compounds that contained different polycyclic cages as ancillary fragments, including norborna(e)ne-derived (**13–16**) or 1-pentylbicyclo[2.2.2]octane-based (**17**) units (group (iii)).

The toxicity of **1–17** was first examined against confluent SK-N-BE2-M17 neuroblastoma cells (M17 cells), with this PD-relevant cell type showing a high tolerance to all compounds at 100  $\mu$ M, as measured by the 3-(4,5-dimethylthiazol-2-yl)-2,5-diphenyltetrazolium bromide (MTT) assay and the lactate dehydrogenase (LDH) assay (Fig. 2a, b). As conjugates of non-toxic DFOB, the low toxicity of this class of compound was predicted, and was consistent with other work.<sup>13,17</sup>

The ability of **1–17** to protect M17 cells that were subject to iron-mediated (endogenous) oxidative damage catalyzed by exogenous 1,1'-dimethyl-4,4'-bipyridinium (paraquat, PQ) or  $H_2O_2$  was measured using the MTT and LDH assays. Two treatment formats (pre-treatment, post-treatment) were examined. In the pre-treatment format, the cells were first incubated with the compound (2 h), excess compound was removed with washing, and the cells were subsequently subject to an oxidative insult from incubation with either PQ or  $H_2O_2$ . This could be considered a representation of prophylaxis, with the compounds designed to remove iron to mitigate iron-mediated PQ or  $H_2O_2$  damage. From a technical vantage, this format was more readily controlled and gave more consistent results across both assays (MTT, LDH) and both oxidants (PQ,  $H_2O_2$ ). The post-treatment format involved incubating the cells with PQ (2 h) or  $H_2O_2$  (1 h), followed by addition of the compound into the medium for a further 24 h. This latter format could arguably represent a more realistic model of the use of iron chelating compounds in PD, with symptoms already present from oxidative insults to the brain. This second format could present a significant challenge for rescue, due to the application of compounds to cells that were already damaged.

Of the compounds in group (i) (**1–7**), **1–3** and **5** gave significant protection in the pre-treatment format, as measured using the MTT assay for the PQ insult (Fig. 2c), with protection indicated as a result occurring above the dotted line, and the LDH assay (Fig. 2d), with protection reflected as a result occurring below the dotted line. The pattern of protection was reasonably well matched between the use of PQ (Fig. 2c, d) or  $H_2O_2$  (Fig. 2e, f) as the insult. The protection of these compounds was significantly greater than that afforded by DFOB, which strongly supported the broader design concept of the use of relatively hydrophobic DFOB-adamantyl and/or polycyclic cage-based conjugates with improved cell membrane carriage for sequestration of intracellular Fe(III). In the post-treatment format, the MTT assay showed **1–5** were protective with the PQ insult (Fig. 2g) and **1** and **3–5** with the  $H_2O_2$

insult (Fig. 2i), with the level of protection less than that afforded in the former system. The results from the parallel LDH assay were less informative (Fig. 2h, j), which was likely due to the comprised integrity of the M17 cells already challenged with PQ or  $H_2O_2$ . Compounds that contained ancillary fragments as deconstructed units of the adamantyl group, **6** and **7** were generally not active, which suggested the structural integrity of the adamantyl group was important for activity, with the methyl-substituted adamantyl variants (**1–3**) generally more active than the unsubstituted parent (**4**).

Of the group (ii) compounds (**8–12**), the bromo-adamantyl-based compounds (**9–10**) were not protective. The performance of the other compounds in this group were variable across the two assay formats. The hydroxyl-substituted adamantyl-acetyl-based **11** was effective in the pre-treatment format, with the chloro-adamantyl-based **8** and the *para*-nitrophenyl-substituted adamantyl-based **12** showing variable performance.

Of the group (iii) compounds (**13–17**), **13** and **14** performed poorly and at similar levels, as expected for geometric isomers. Compounds **15** and **16** showed variable protection. The 1-pentylbicyclo[2.2.2]octane-based **17** showed the most consistent protection across the MTT and LDH assays, and the two different assay formats. The methyl-substituted adamantyl compounds **1–3** and the alkyl-substituted bicyclo[2.2.2]octane compound **17** performed consistently above the norborna(e)ne-based compounds. The protective capacity of the norborna(e)ne-based cages could potentially be improved with further alkylation to approach the number of methylene groups (calculated in the absence of the pendant carboxylate group) present in the ancillary units of **1–3** ( $C_{12}$ – $C_{13}$ ) and **17** ( $C_{13}$ ). These data supported the posit of a relationship between hydrophobicity and the protective potential for these compounds in these *in vitro* experimental models of PD.

The top-performing candidates from this first screen (**1–3**, **5**, **17**) were subject to a dose-dependence study in M17 cells pre-treated with PQ (Fig. 3). The  $EC_{50}$  values estimated from the fitted dose–response curves for the MTT data were: **1** (3.4  $\mu$ M), **2** (5.8  $\mu$ M), **3** (9.8  $\mu$ M), **5** (30  $\mu$ M) or **17** (10  $\mu$ M). No protective effect was observed for DFOB up to 1 mM, and an  $EC_{50}$  value could not be calculated. Due to the error in the data, the global  $EC_{50}$  value of 10  $\mu$ M was ascribed to **1–3** and **17**.

The activity of **1–17** in two other models of oxidative stress were examined. In the first model, the M17 cells were pre-treated with  $FeCl_3$ , followed by PQ, and then treated with DFOB or **1–17** (Fig. 4). Pre-loading the cells with exogenous iron would be expected to exacerbate the oxidative stress in the presence of PQ. In this system, **1–6**, **8**, **14** and **15** gave protection in the MTT assay (Fig. 4a), with results correlating in the LDH assay for **1–4**, **6**, **14** and **15** (Fig. 4b). Compound **12** was protective in the LDH assay.

In the second model of oxidative stress, **1–17** were assessed in primary astrocytes that had been pre-incubated with buthionine sulfoximine (BSO) to deplete levels of the endogenous antioxidant glutathione. In this second *in vitro* cell type, **1–6, 8, 9, 12** and **17** showed significant protective capacity in the MTT assay, compared to vehicle (Fig. 5a), with results in the LDH assay (Fig. 5b) correlating for **1–4, 6, 8, 12** and **17**.

Analysis of all the *in vitro* cell models showed **1–3** and **17** were the most effective across all models (Fig. 6). A general trend in a decrease in activity was evident as the methyl groups were removed from the adamantyl cage, and as the adamantyl cage was dismantled (**1–7**). The halogenated adamantyl-based compounds (**8–10**) were generally poorly active, with chlorinated **8** ranked higher than brominated **9–10**. The norborna(e)ne- (**13–16**) based compounds were less active than the methyl-substituted adamantyl-based group (**1–3**). The 1-pentylbicyclo[2.2.2]octane-based ancillary group (**17**) showed activity in range with **1–3**, which suggests the lipophilicity of the polycyclic cage motif is a determinant of activity. Excluding the carboxylic acid group, the ancillary fragments **13–16** comprise 7–8 carbon atoms. Fragment **17** comprises 13 carbon atoms, in range with fragments **1–3** (12–13 carbon atoms). The correlate between lipophilicity and activity was consistent with the poor activity of hydroxylated **11**, which was relatively water soluble ( $\log P = 0.15$ ). Compounds **5** and **12** performed well in many models, but were more variable. This suggests that other ancillary fragments, such as the *p*-nitrophenyl-substituted adamantyl group (**12**), may have some therapeutic utility and highlights the importance of using more than one *in vitro* cell model for ranking compound performance.

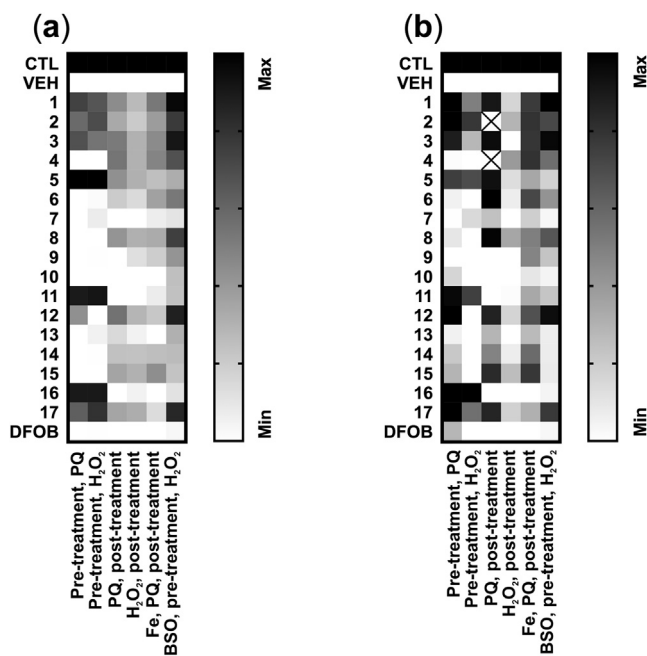


**Fig. 6.** Heatmap of cell viability as measured by MTT assay (a) or LDH assay (b) of data presented in Figs. 2, 4 and 5. M17 cells were treated with DFOB (100  $\mu\text{M}$ ) or **1–17** (100  $\mu\text{M}$ ), then 1 mM PQ (Pre-treatment, PQ) or 1 mM  $\text{H}_2\text{O}_2$  (Pre-treatment,  $\text{H}_2\text{O}_2$ ); or treated with 2 mM PQ or 0.8 mM  $\text{H}_2\text{O}_2$ , then DFOB (100  $\mu\text{M}$ ) or **1–17** (100  $\mu\text{M}$ ) (PQ, post-treatment or  $\text{H}_2\text{O}_2$  post-treatment, respectively); or treated with 200  $\mu\text{M}$   $\text{FeCl}_3$ , then 1 mM PQ, then DFOB (100  $\mu\text{M}$ ) or **1–17** (100  $\mu\text{M}$ ) (Fe, PQ, post-treatment). Primary astrocytes were treated with BSO (1 mM), then DFOB (10  $\mu\text{M}$ ) or **1–17** (10  $\mu\text{M}$ ), then 200  $\mu\text{M}$   $\text{H}_2\text{O}_2$  (BSO, pre-treatment,  $\text{H}_2\text{O}_2$ ). Data normalized to minimum viability (VEH: cells treated with stressor but no compound) and maximum viability (CTL: cells treated in the absence of compound or stressor). Data for cells marked with a cross were not obtained.

The ability of a selected number of candidates to remove intracellular iron was examined using primary astrocytes that had been iron loaded with ferric ammonium citrate (FAC) prior to incubation with the compounds or with vehicle (Fig. 7). Compounds **1, 2, 17** were assessed in this system, together with DFOB and compound **7**, with the latter selected as a negative control due to its poor performance in both the M17 and primary astrocyte cell systems. Compound **2** and **17** resulted in a significant measure of depleted iron, compared to FAC-loaded cells treated with vehicle. DFOB was ineffective at depleting iron levels. In an unexpected result, **7** was equally effective with **2**

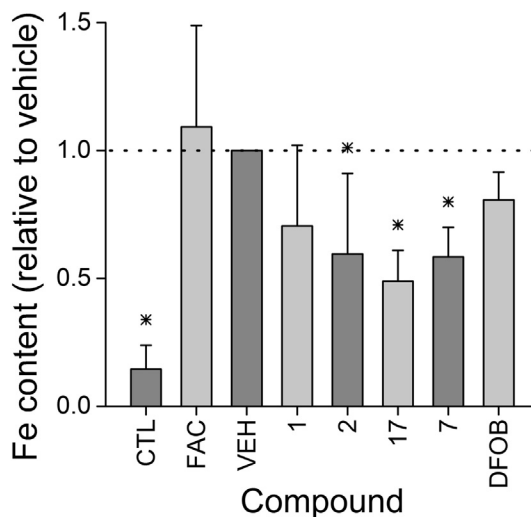


**Fig. 7.** Primary astrocytes were incubated for 2 h in the presence (FAC) or absence (CTL) of FAC (125  $\mu\text{M}$ ) to load cells with iron before the medium was aspirated and replaced with medium containing vehicle (VEH), DFOB (100  $\mu\text{M}$ ) or a **1, 2, 7** or **17** (100  $\mu\text{M}$ ) for a further 2 h incubation. The cells were processed and analyzed for Fe content by ICP-MS. Values below the dotted line corresponded with compounds that removed cell-associated Fe as compared to vehicle. Data are presented as averages  $\pm$  standard deviation of 4 independently prepared cell cultures, with  $^*p < 0.05$  compared to vehicle (dotted line).

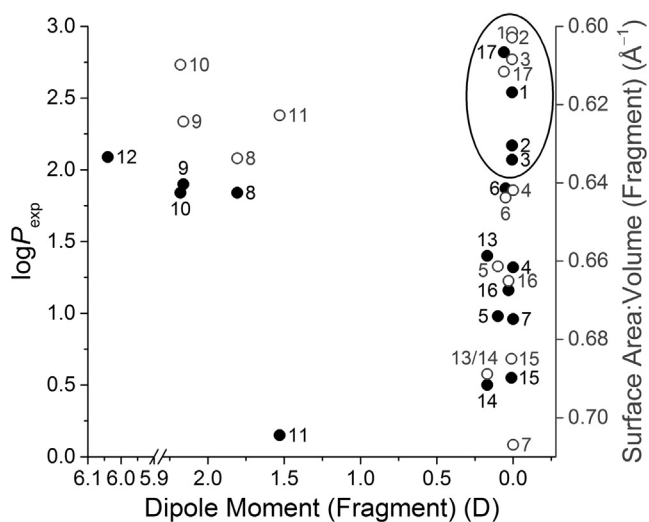


**Fig. 8.** Plot of the calculated dipole moments of the ancillary fragments of **1–17** versus the experimental  $\log P$  values (closed circles) of compounds **1–17**, or calculated surface area:volume ratios of the ancillary fragments (open circles) of **1–17**. The compounds that performed best in the iron-induced oxidative stress cell models are bound by the oval.

and **17** at depleting iron levels. It could be possible that **7** was removing iron located at the membrane surface which remained cell-associated after the washing step. The  $\log P$  value of **7** ( $\log P = 0.96$ ) would indicate an ability to associate with the cell membrane, unlike water soluble DFOB. It could be that the protective capacity is dependent upon the chelation of specific sub-cellular pools of iron, which cannot be assessed by quantitation of bulk iron content.

The results showed that across two *in vitro* cell types (M17, primary astrocytes) and several types of oxidative challenges, the most consistent top-performing compounds featured a poly-methyl-substituted adamantyl or -adamantyl-acetyl-based ancillary group conjugated to DFOB (**1–3**), or contained a 1-pentylbicyclo[2.2.2]octane-based ancillary group (**17**). The activity of these compounds could be correlated with relatively high  $\log P$  values (both experimental and calculated). One other facet for **1–3** was the high level of symmetry and the spherical nature of the ancillary fragments, as reflected by the close-to-zero dipole moments and the relatively small surface area:volume ratio (0.60–0.61). A plot of the dipole moment of the ancillary fragment versus experimental  $\log P$  values (Fig. 8, black) or the surface area:volume ratio of the ancillary fragment (Fig. 8, grey) shows the most consistently performing compounds (**1–3**, **17**) clustered in a domain bound by  $\log P_{exp}$  2.07–2.82, dipole moment (ancillary fragment) 0.01–0.06, and surface area:volume (ancillary fragment) 0.60–0.61. Other studies have shown a trend towards spherically shaped compounds having superior ability to cross the BBB, compared to rod shaped and/or branched-type compounds.<sup>20,21</sup> This work has provided a guiding structure-activity relationship for this class of compound and shown that **1–3** and **17** could reasonably move to testing in *in vivo* models of PD.

## Acknowledgment

Funding from the NHMRC (APP1061761) is kindly acknowledged.

## A. Supplementary data

Supplementary data associated with this article can be found, in the online version, at <http://dx.doi.org/10.1016/j.bmcl.2017.03.001>.

## References

1. Cairo G, Bernuzzi F, Recalcati S. *Genes Nutr.* 2006;1:25.
2. Halliwell B. *Drugs Aging.* 2001;18:685.
3. Olivieri NF, Brittenham GM. *Blood.* 1997;89:739.
4. Weatherall DJ. *Blood.* 2010;115:4331.
5. Sankaran VG, Weiss M. *J Nat Med.* 2015;21:221.
6. Zecca L, Youdim MB, Riederer P, Connor JR, Crichton RR. *Nat Rev Neurosci.* 2004;5:863.
7. Dorsey ER, Constantinescu R, Thompson JP, et al. *Neurology.* 2007;68:384.
8. Devos D, Moreau C, Devedijan JC, et al. *Antioxid Redox Signal.* 2014;21:195.
9. Telfer TJ, Gotsbacher MP, Soe CZ, Codd R. *ACS Chem Biol.* 2016;11:1452.
10. Ejje N, Soe CZ, Gu J, Codd R. *Metallomics.* 2013;5:1519.
11. Alta ECP, Goswami D, Machini MT, Silvestre DM, Nomura CS, Espósito BP. *Biometals.* 2014;27:1351.
12. Goswami D, Teresa MM, Silvestre DM, MNomura CS, Esposito BP. *Bioconjugate Chem.* 2014;25:2067.
13. Liu J, Obando D, Schipanski LG, et al. *J Med Chem.* 2010;53:1370.
14. Liu J, Obando D, Liao V, Lifa T, Codd R. *Eur J Med Chem.* 2011;46:1949.
15. Wanka L, Iqbal K, Schreiner PR. *Chem Rev.* 2013;113:3516.
16. Stockdale TP, Williams CM. *Chem Soc Rev.* 2015;44:7737.
17. Liddell JR, Obando D, Liu J, et al. *Free Radic Biol Med.* 2013;60:147.
18. Yamagami C, Ogura T, Takao N. *J Chromatogr.* 1990;514:123.
19. Yamagami C, Araki K, Ohnishi K, et al. *J Pharm Sci.* 1999;88:1299.
20. Pajouhesh H, Lenz GR. *NeuroRx.* 2005;2:541.
21. Fong CW. *J Membrane Biol.* 2015;248:651.